RESEARCH ARTICLE OPEN ACCESS

High Molecular Weight Thermally Stable Poly (Sodium Methacrylate) / Magnetites Nanocomposites Via Emulsion Polymerization

Rasha A. El-Ghazawy[a,] Ayman M. Atta[b], Ashraf M. El-Saeed[a], Ahmed E.S. Abdelmgied[c] and Nivin Basiouny

[a]Petroleum Application Department, Egyptian Petroleum Research Institute, Nasr City 11727, Cairo, Egypt.
[b]Surfactants research chair, Chemistry Department, College of Science, King Saud University, P.O. 2455, Riyadh - 11451, Saudi Arabia
[c] Menoufia University, Faculty of Science, Chemistry Department, 32511, Menoufia, Egypt.

ABSTRACT
Core/shell type magnetite nanocomposites (MN) were synthesized using sodium methacrylate (NMA) monomer. Functionalized and bare magnetite nanoparticles were prepared by conventional co-precipitation method giving particles with 3-10 nm in diameter. Microemulsion polymerization was used for constructing core/shell structure with magnetite nanoparticles as core and poly (sodium methacrylate) as shell. Chemical structure and morphology of the synthesized PNMA/magnetite nanocomposites were investigated using FTIR and TEM, respectively. The synthesized nanocomposites show effective encapsulation of different treated magnetite nanoparticles in the polymer matrix and exhibited good thermal stability. Such magnetite nanocomposites with high molecular weight and thermal stability have potential application in enhanced oil recovery application.
Keywords-Nanocomposites, TEM, modified magnetite nanoparticles, thermal stability.

I. INTRODUCTION

Water-soluble polymers have a very broad range of industrial applications. They are used primarily to disperse, suspend (thicken and gel), or stabilize particulate matter. These functions make water-soluble polymers suitable for a wide variety of applications including water treatment, paper processing, mineral processing, formulation of detergents, textile processing, the manufacture of personal care products, pharmaceuticals, petroleum production, enhanced oil recovery and formulation of surface coatings. Water-soluble polymers for enhanced oil recovery (EOR) applications have been successfully implemented in various oil fields with a purpose of enhancing the thickening properties of the displacing fluid. Such polymers enable injected water to better match the viscosity of reservoir oil, which improves the water penetration into the rock pores to improve oil production. However, given the harsh conditions present in most oil reservoirs, water-soluble polymers should withstand high temperatures (>70 ◦C), long injection times (at least 12 months), high salt concentration, and others1. Thus polymers for EOR should mainly attain high molecular-weight and thermal stability.

The water-in-oil (W/O) emulsion polymerization process shows superior characteristics2 such as the low viscosity of the dispersion, ease removal of the reaction heat3 and the high molecular weight of the obtained polymer4 etc. In addition, it is an attractive reaction system as the polymerization process is also prospective to prepare particles in nano-scale. Miniemulsion polymerization is considered as one of the best methods to prepare

composite particles. Owning to the character of the droplet nucleation, inorganic or organic particles or other hydrophilic or hydrophobic additives could be encapsulated inside or on the surface layer of the latex particles depending on the location of additives after miniemulsification. For example, polystyrene (PSt)/Fe3O4 composite particles were synthesized by the miniemulsion polymerization of styrene in the presence of metal nanoparticles5. Zhou et al.6 synthesized SiO2/poly(styrene-co-butyl acrylate) nanocomposite microspheres with various morphologies (e.g., multicore-shell, normal core–shell, and raspberry-like) via the miniemulsion polymerization of styrene and butyl acrylate. Titanium dioxide/ copolymer composite nanoparticles were prepared by miniemulsion copolymerization of styrene and butyl acrylate7.

On the other hand, organic/inorganic nanocomposite materials have been extensively studied in the last few decades as they provide the possibility for enhanced functionality and multifunctional properties in contrast with their more-limited single-component counterparts8,9. A main advantage of polymer nanocomposites is

retaining the inherent properties of nanoparticles as well as providing high stability, processability and other interesting improvements of polymer matrix depending on nanoparticles – polymer interactions. Also, nanocomposite performance requires a homogeneous distribution of nanoparticles within polymer matrices -avoiding the formation of agglomerates- which is a general problem in their preparation.

Zolfaghari et al.10 haveprepared nanocomposite type of hydrogels (NC gels) by crosslinking the polyacrylamide/montmorillonite (Na- MMT) clay aqueous solutions with chromium (III). These NC gels were effectively used for water shut-off and as profile modifier in enhanced oil recovery (EOR) process during water flooding process.In a recent research Tongwa et al.11have synthesized nanocomposite hydrogel from just polymer and clay without the use of conventional organic crosslinkers. It was found that these hydrogels show surprising mechanical toughness, tensile moduli, and tensile strengths.

This article aims to prepare water soluble poly (sodium methacrylate) / magnetite nanocomposites with high thermal stability and suitable molecular weight that matching with enhanced oil recovery application. In this respect, non-functinalized and two different functionalized magnetite nanoparticles were prepared. In situ synthesis approach was used for preparing nanocomposites using microemulsion polymerization technique. The effect of magnetite type on thermal stability and morphology of poly (sodium methacrylate)/magnetite nanocomposites were evaluated using thermogravimetric analysis and transmission electron microscopy.

II. EXPERIMENTAL

2.1. Materials

Ferrous chloride tetrahydrate, ferric chloride hexahydrate, iron tri(acetyl acetonate), 1,2-tetradecandiol, oleic acid (OA), oleylamine, benzyl ether, 1,2-dichlorobenzene, dibenzoyl peroxide (BP), N,N,N,N-tetramethy lethylenediamine (TEMED), toluene, triton X100, decanol were purchased from Aldrich chemical company. Sodium hydroxide,methanol, citric acid (C), N,N`-dimethyl formamide, acetone were obtained from El-Gomhouria chemical company, Egypt

2.2. Nanoparticles synthesis:

Non-functionalized magnetite nanoparticles (G) were prepared by co-precipitation method12. Stoichometric ratio 1:2 of FeCl2.4 H2O and FeCl3.6H2O aqueous solution was drop-wisely added to strong alkaline NaOH solution with strong stirring and under a blanket of nitrogen. The reaction temperature was raised to 80^0 C and continued for 30 min. The precipitated Fe3O4 was repeatedly washed by de-ionized water till pH of 7.

Functionalized oleic acid coated magnetite nanoparticles (OG) were prepared as depicted by Sun et al.[13]. Iron tri(acetyl acetonate) (2 mmol), 1,2-tetradecandiol (10mmol), oleic acid (6 mmol), oleylamine (6 mmol) and benzyl ether (20 ml) were mixed under a constant flow of nitrogen. The mixture was heated gradually to 100^0 C and kept at this temperature for 45 min. The temperature was raised to 200^0 C for 2h and then to 300^0 C for 1h. After cooling the reaction to room temperature, 40 ml of methanol was added where a black precipitate was formed. The formed oleic acid coated magnetite was kept dispersed in hexane till required. Excess methanol was used to precipitate oleic acid coated magnetite which was centrifuged at 20000rpm for 10 min and dried at 80^0 C for 20 min.

Citric acid coated magnetite nanoparticles (CG) were prepared by replacing oleic acid and oleyl amine moieties by citric acid. The procedures are briefly described by Sun et al.13. One gram of citric acid was added to 120 mg of the prepared oleic acid and oleyl amine coated nanoparticles dispersion in 1:1 mixture of 1,2-dichlorobenzene and N,N`-dimethyl formamide. The mixture was heated to 100^0 C for 24 h and after cooling the nanoparticles were precipitated by 40 ml ethyl ether and separated. Free citric acid was repeatedly washed by acetone and the coated particles were dried at 80^0 C for 20 min.

2.3. Preparation of poly (sodium methacrylate) / magnetite nanocomposites:

In situ polymerization of sodium methacrylate monomer as a host and one type of the prepared nanoparticleswas performed. The nanoparticles were separately directly dispersed intoaqueous phase in case of non-functionalized (bare) magnetite (G) and citric acid coated magnetite nanoparticles (CG) whereas oleic acid coated magnetite nanoparticles (OG) were dispersed in oil phase. Sodium methacrylate (NMA) was polymerized in an inverse w/o microemulsions using dibenzoyl peroxide (BP) and N,N,N,N-tetramethylethylenediamine (TEMED) as a redox pair initiation system. The typical w/o microemulsion composition was 61.7 wt.% toluene, 14.5 wt.% triton X100, 4% wt.% decanol, 14.18 wt.% H2O and 5.62 wt.% NMA.A second coat of polymer was polymerized in a second step using additional quantity of NMA equivalent to that previously added. 0.01% of ammonium persulfate (APS), 0.03% TEMED and 0.01% N,N- methylenebisacrylamide (MBA) as crosslinker were added to the microemulsion system. Only PNMA/OG NCs were

crosslinked with different MBA weight ratios 0.01, 0.1 and 5%. The microemulsion system was firstly sonicated for 1h where the samples were submerged in ice-cooled bath. The as-prepared microemulsion was transferred into a 100 ml glass reactor equipped with nitrogen inlet and the reaction was performed at 30□C with constant stirring speed at 500 rpm and for 24h. The polymerization yields brownish inverse latex containing polyNMA/magnetite particles. The particles were isolated by distilling most of toluene and water under vacuum and then dried in an oven at 50□C for 24 h. Excess methanol was used to remove the adsorbed triton from the particles and again the particles were dried at 50□C for 24 h.

2.4. Characterization

Bare and coated iron oxide particles viz., G, OG and CG were characterized using fourier-transform infrared spectroscopy (FTIR) [Nicolet iS10 FT-IR Spectrometer, Thermo Fischer Scientific Co.,]. Type of prepared functionalized and non-functionalized iron oxides and their particle sizewere estimated using X-ray powder diffractometry [X'pert PRO PAN analyst]. Different types of magnetites and their corresponding nanocomposites were observed using high resolution transmission electron microscopy (HRTEM) [Jeol 2010 F]. The average molecular masses and molecular mass distributions of non-crosslinked poly (sodium methacrylic acid) polymerized with different initiator (BP) concentrations were determined using gel permeation chromatography (GPC, Agilent 1100 series, Germany, Detector: Refractive Index). GPC analysis were performed using water solvent and polyethylene oxide/glycol standard, PL aquagel-OH 7.5 mm, 30um pore type, 8um particle size and PL aquagel-OH 7.5 mm, 50um pore type, 8um particle size, in series for Mw from 100-1250000 g/mol. Thermal degradation of the polymeric nancomposites was conducted from 30 to 1000 □C with a heating rate of 10 □C/min, under dynamic flow of nitrogen using differential scanning calorimeter(DSC) (Simultaneous DSC-TGA, Q 600 STD, USA).

III. RESULTS AND DISCUSSION

A critical step in the preparation of the nanocomposite particlescontaining dispersed iron-oxide nanoparticles is the preparationof a stable suspension of iron-oxide nanoparticles in sodiummethacrylate monomer. In addition, hydrophilicity/hydrophobicity of iron-oxidenanoparticles surface mayaffect theircompatibility and dispersability with the hydrophilic poly(sodium methacrylate). This may lead to encapsulation of inorganic particles inside or on the surface layer of latex particles.Non-functionalized iron-oxide nanoparticles arehydrophilic due to the presence of surface –OH groups. Thesegroups are formed due to the hydration of the nanoparticles surfaces'during the synthesis in the aqueous solution[14]. Long-chainfatty acids are usually employed to hydrophobize the iron-oxidenanoparticles' surfaces[15]. These fatty acids are bonded to theiron-oxide nanoparticles' surfaces through a coordinative bondbetween the carboxyl group of the acid and the iron cations[16].The fatty acid's tail, which is oriented outward from the iron-oxide nanoparticles' surfaces, provides the hydrophobic character of the nanoparticles. From among the different long-chain fatty acids, it is oleic acid that is mainly used for the preparation of stable suspensions of iron-oxide nanoparticles in non-polar solvents such ashydrocarbons[15].

3.1. FTIR of G, OG and CG

The FT-IR spectrum of the synthesized Fe_3O_4 magnetite nanoparticles (G) is presented in Figure1. The strong absorption band at 636 $cm^{-1}$is assigned to the vibrations of the Fe-O bond, which confirms the formation of Fe nanoparticles. This absorption value is higher than previously reported for Fe-O in bulk Fe_3O_4 where the characteristic absorption band was appeared at 570 and 375 cm^{-1}wavenumber[17]. This may be due to the breaking of the large number of bands for surface atoms, resulting rearrangement of localized electrons on the particle surface and the surface bond force constant increases as Fe_3O_4 is reduced to nanoscale dimension, so that the absorption bands shift to higher wavenumber[18]. The broad bands at 3361cm^{-1} and 1620cm^{-1} are assigned to O-H stretching and bending vibrations of water respectively, which is present on the surface of the iron oxide nanoparticles[18].

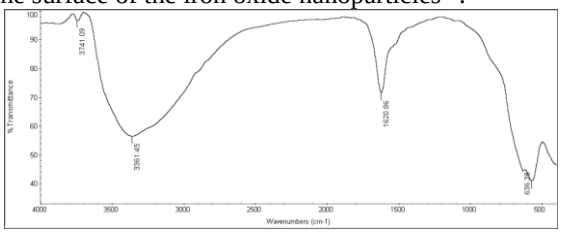

Figure 1: FTIR spectrum for magnetite

To understand the adsorption mechanism of the OA on thesurface of Fe_3O_4 nanoparticles, Fourier transform infraredmeasurements were carried out on pure oleic acid and Fe_3O_4 nanoparticles coated with OA. Figure2a for pure oleic acid shows broad feature between 2700 and 3200 cm^{-1} is undoubtedly due to O-H stretching of carboxylic acid group overlapped with two sharp bands at 2942 and 2858 cm^{-1}that are attributed to asymmetric and symmetric CH_2 stretching, respectively. The intense peak at 1712 cm^{-1} is derived from the existence of carbonyl stretching whereas the band at 1289 cm^{-1} is assigned for C-O

stretching. In-plane and out-of-plane bands for O-H appears at 1458 and 938 cm^{-1}, respectively. Figure 2b reveals FTIR spectrum for Fe_3O_4 nanoparticles coated with oleic acid. It shows two sharp bands at 2924 and 2854 cm^{-1}that attributed to the asymmetric CH_2 stretch and the symmetric CH_2 stretch, respectively. The intense peak at 1741 cm^{-1} was derived from the existence of the C=O stretch, and the band at 1239 cm^{-1} exhibited the presence of the C–O stretch of oleic acid. The extremely broad stretching of O–H absorption appeared in the region from 3100 - 3600cm^{-1}. The oleic acid surfactant molecules in the adsorbed state onto magnetite were subjected to the field of solid surface. As a result, the characteristic bands of oleic acid are shifted to a lower frequency region indicating that the hydrocarbon chains in the monolayer surrounding iron nanoparticles are in a closed pack crystalline state[19].It can be observed that the characteristic C=O band (present at 1712 cm^{-1} for pure oleic) is absent with the appearance of two new bands at 1618 and 1638 cm^{-1} characteristic to asymmetric and symmetric carboxylate stretching. These results revealedthat oleic acid were chemisorbed onto the Fe_3O_4 nanoparticlesas a carboxylate with both oxygen atoms coordinated symmetrically to Fe atoms. Magnetite formation can be confirmed through the presence of 605 and 472 cm^{-1}bands assigned to stretching and torsional vibration modes of the magnetite.

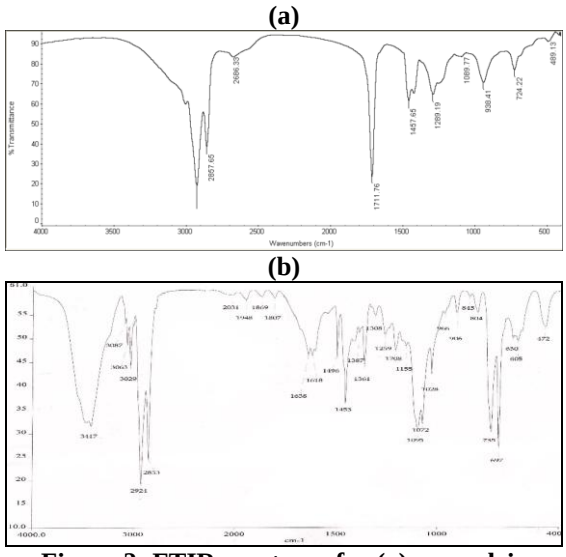

Figure 2: FTIR spectrum for (a) pure oleic acidand (b) OG.

Figure 3 (a-b) show the FTIR spectrum of pure citric acid and magnetite particles coated with citric acid (CG), respectively. Regarding figures 3 (a-b), there is a significant difference between both spectra. Both spectra show a large, broad and intense band in region from 2500 to 3500 cm^{-1} assigned to the structural OH groups of molecular citric acid. Citric acid spectrum shows sharp band at 1719 cm^{-1}assignableto the C=O vibration (symmetric stretching) from the COOH group of citric-acid (CA). An intense band at about 1626 cm^{-1} for the ferromagnetic phase coated with citric acid is observed in Figure 1b with diminished intensity of 1718 cm^{-1} band. This feature reveals the binding of a CA radical to the magnetite surface. Ferromagnetic coated phase (Figure3b) shows a band at1376 cm^{-1}which is assigned to the asymmetric stretching of C─O of COOH group. Near IR bands at584 and 637 cm^{-1}can be assigned stretching and torsional vibration modes of the magnetite. Thus, one may suppose that citric acid binds chemically to the magnetite surface by carboxylate chemisorptions.

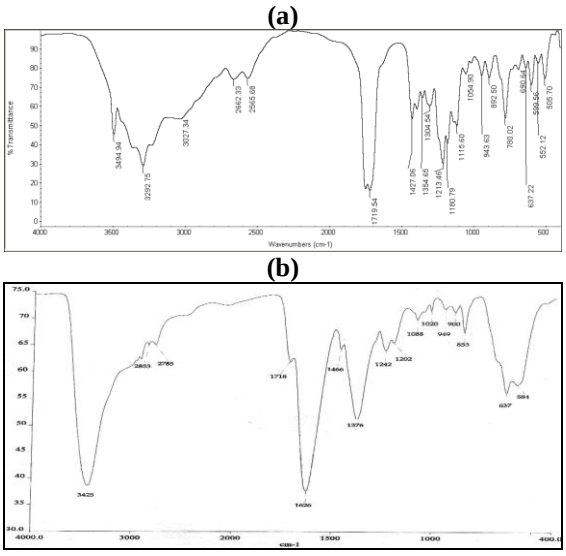

Figure 3: FTIR spectrum for (a) pure citric acid and (b) CG.

3.2. XRD for G, OG and CG

G, OG and CG nanoparticles were analyzed using XRD and their diffraction patterns are shown in Figures4-6, respectively. It is clear from graphs that only the phase of Fe_3O_4 is detectable where the XRD patterns show that the samples are pure Fe_3O_4 without impurity phases and match well with the standard pattern of Fe_3O_4 [ref. code 00-002-1035]. There is no other phases such as $Fe(OH)_3$ or Fe_2O_3, which are the usual co-products in a chemical co-precipitation and oxidative hydrolysis methods. For CG as an example, the peaks at 2θ equal to 29.9□, 35.3□, 43.2□, 53.5□, 57.1□, and 62.7□ can be indexed as (220), (311), (400), (422), (511), and (440) lattice planes of magnetite, respectively [ref. code 00-002-1035]. In all cases, the spectra consist

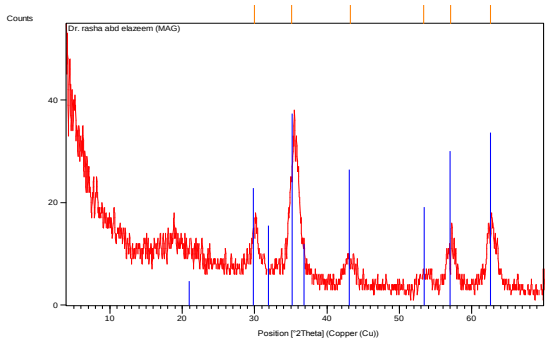

Figure 4: XRD spectrum of G.

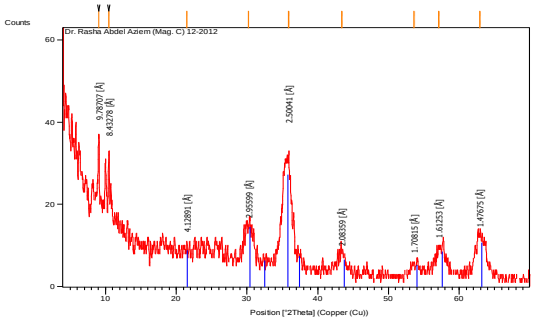

Figure 5: XRD spectrum of OG

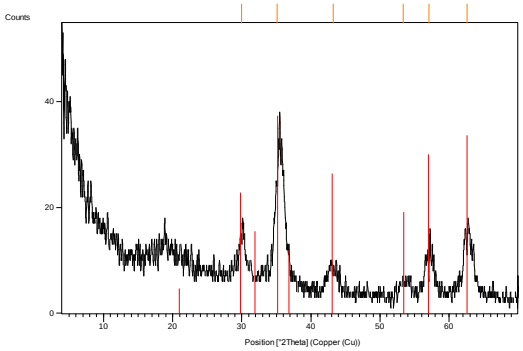

Figure 6: XRD spectrum of CG.

of broad peaks that can be ascribed to the cubic structure. From the broadening of the diffraction peaks, the average core size of the particles can be evaluated from Scherrer equation (Eq. 1).

$$L = 0.94\lambda/B\,(2\theta)\cos\theta \quad (1)$$

where, L is equivalent to the average core diameter of the particles, λ is the wavelength of the incident X-ray, B(2θ) denotes the full width in radian subtended by the half maximum intensity width of the power peak, for instance (311), and θ corresponds to the angle of the (311) peak. Using the above equation and the peak at 100% relative intensity, the particle size of G, OG and CG are 8, 6.7 and 8 nm, respectively.

3.3. TEM for magnetites and nanocomposites

The morphologies of the prepared magnetites (G, OG and CG) and their nanocomposites with poly sodium methacrylate were investigated by TEM and shown in Figures (7-9), respectively. Figure 7 (left) shows the TEM image of non-functionalized magnetite. It can be observed that magnetite particles are in nanometer range. The diameter of Fe_3O_4 nanoparticles was about 3.5 - 10nm.Figure7 (right) for G nanocomposite shows slightly larger nanoparticles. Both G and its nanocomposite show irregular particle shape. However, TEM for G and its nanocomposite revealed that the nanoparticles were effectively encapsulated in the polymer matrix. The nanoparticles are visible as darker dots inside the brighter polymer matrix.

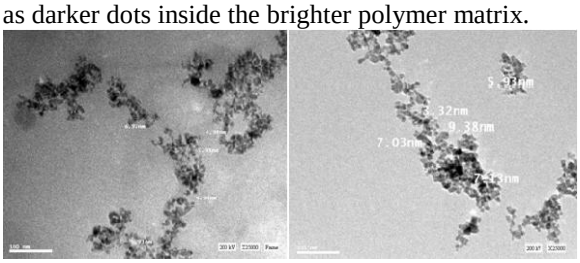

Figure 7: TEM image for non-functionalized magnetite (G) (left) and poly sodium methacrylic acid/ G nanocomposite (right).

Figure8 (left) shows TEM micrographs of magnetite nanoparticles coated with oleic acid. It can be seen that magnetite nanoparticles assemble very well. Each particle is separated from its neighbors by the organic ligand shell. The particle size is about 5-9 nm with main cubic shape. Figure 8 (right) for OG nanocomposite show larger particle size reaching about 20 nm. It also shows some agglomeration. This increase in particle size may be attributed to the hydrophobic nature of oleic acid coated magnetite in contrast with hydrophilic poly sodium methacrylate.

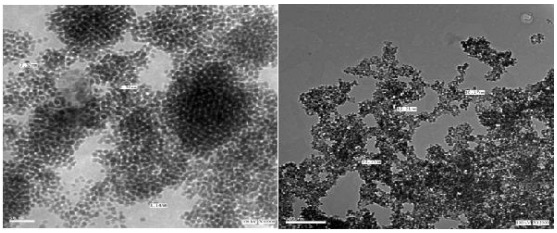

Figure 8: TEM image for oleic acid functionalized magnetite (OG) (left) and poly sodium methacrylic acid/ OG nanocomposite (right)

TEM of citric acid coated magnetite is shown in Figure9 (left). Good dispersion of nanoparticles is observed from TEM image with no agglomeration. The particle size is in the range of 5-8 nm. CG poly sodium methacrylate nanocomposite TEM (Figure9 (right)) shows well-spaced coated CG particles assemblies.

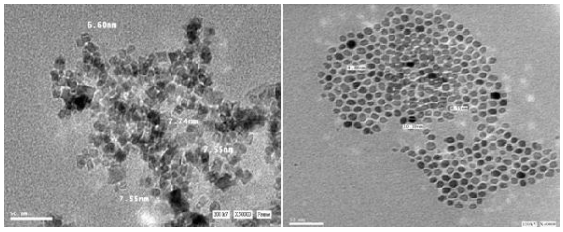

Figure 9: TEM image for citric acid functionalized magnetite (CG) (left) and poly sodium methacrylic acid/ CG nanocomposite (right)

However, the estimates of the size from the XRD are in good agreement with the measurements from TEM images.

3.4. GPC analysis for uncrosslinkerd polymers

The number and weight averages of the molecular masses andtheir distribution in the linear polymers of different PNMAs prepared using microemulsion polymerization –described in experimental section- with different BP concentrations (m_{BP}/m_{NMA} % = 1.6x $x10^{-3}$, 8 x 10^{-4}, 4 x 10^{-4}, 4 x 10^{-4}, 2 x 10^{-4} or 1 x 10^{-4})were obtained using GPC (Table 1). The data in Table 1 indicate that the prepared PNMAs are of low polydispersity with increased molecular weight upon decreasing the BP concentration reaching 1.1 x 10^{6} g/mol for 1 x 10^{-4} BP weight % (see Figure10). This concentration was selected for the preparation of all NCs through the article.

Table 1: GPC data for PNMA prepared at different BP concentrations

BP concentration	M_w (g/mol)	M_n (g/mol)	Polydisp-ersity
1.6 x 10^{-3}	6.5 x 10^{5}	3.96 x 10^{5}	1.6
8 x 10^{-4}	7.9 x 10^{5}	3.90 x 10^{5}	2.0
4 x 10^{-4}	3.7 x 10^{5}	1.52 x 10^{5}	2.4
2 x 10^{-4}	1.01 x 10^{6}	4.34 x 10^{5}	2.3
1 x 10^{-4}	1.1 x 10^{6}	4.49 x 10^{5}	2.5

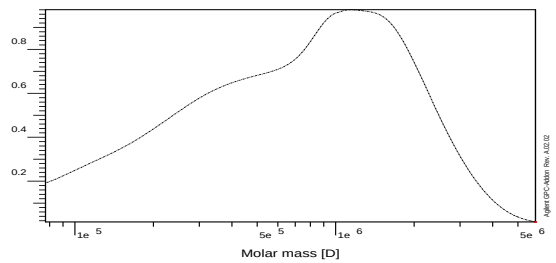

Figure 10: GPC of PNMA prepared by using 1 x 10^{-4} % BP

3.5. TGA for PNMA / magnetite nanocomposites

The influence on magnetite nanoparticles on thermal stability and decomposition behavior of polymer matrix were investigated taking the unfilled PNMA as the reference material. Figure 11 shows thermogrvimetric curve for unfilled crosslinked PNMA using 0.01% MBA. The first weight loss indicates evaporation of water in the temperature range between 50 and 148 □C. This first weight loss indicates that PNMA is hygroscopic as pointed out by McNeill and Zulfiqar[20]. A second weight loss step is observed from 148 to 318 □C that accounts for 82.4% weight loss. The thermograms of nanocomposites (NC) for PNMA/OG prepared at 100/0.5 and 100/5 weight ratios of PNMA: OG ratios crosslinked with 0.01% MBA, are shown in Figures 12-13. One can observe that the thermograms are divided into four steps. The first weight loss process in both cases, in the temperature range 25-185°C, is independent of the NC samples composition and is

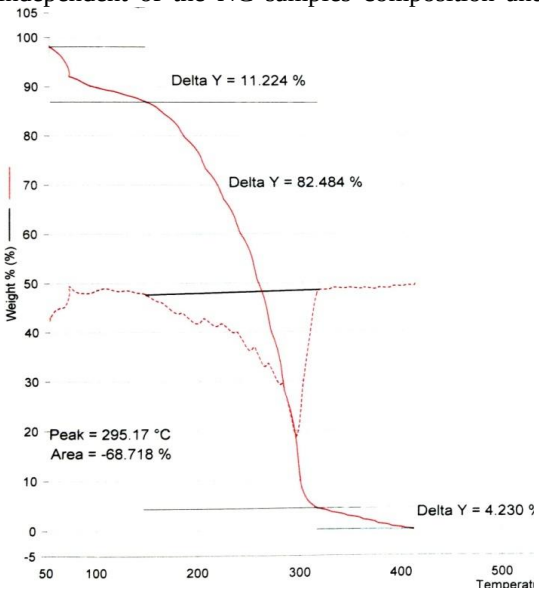

Figure 11: Thermogram for unfilled PNMA

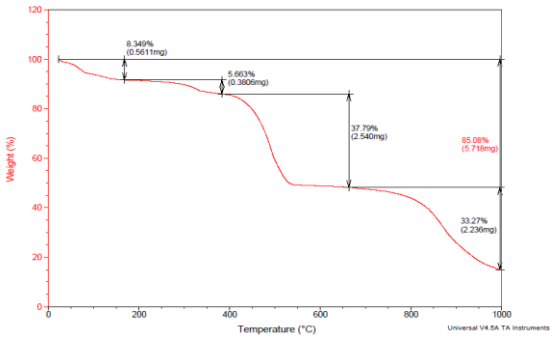

Figure 12: Thermogram for 100/0.5 weight artion of PNMA/Mag-OA and 0.01% MBA

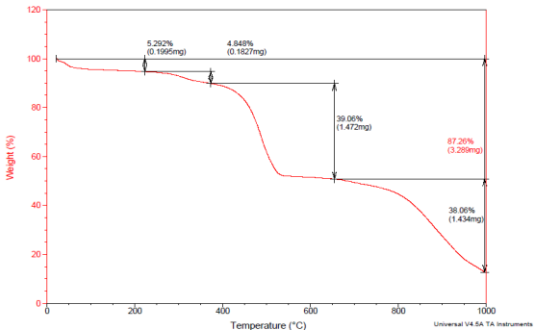

Figure 13: Thermogram for 100/5 weight artion of PNMA/Mag-OA and 0.01% MBA

associated with the loss ofadsorbed water that constitute 5-8 weight % of 100/0.5 and 100/5 weight ratios of PNMA/OG, respectively. For 100/0.5 weight ratio of PNMA/OG NC, the second weight loss processes lies in thetemperature ranges 200-375°C that can beattributed to loss of loosely bonded polymer matrix. The second step for 100/5 weight ratio of PNMA/OGNC shows more stability, it happens at 225-387 □C. In other words, this weight loss process is influenced by the magnetite concentration used for nanocomposites preparation. Both third (400-536 □C) and fourth (661-1000 □C) steps for both nanocomposites show advanced thermal stability of these nanocmposites with reference to unfilled polymer.

Thermograms for nanocomposites prepared at 100/5 weight ratio of PNMA/OG crosslinked with different crosslinker concentrations viz., 0.1 and 5% are shown in Figures14-15. These figures show similar behavior i.e., four decomposition steps. The first step also shows weight loss of about 5% in the temperature range 25-140 □C ascribed for water evaporation for the three crosslinker concentrations. The onset and maximum decomposition rate temperatures for the second step increases upon increasing the crosslinker concentration (225-387, 238-392 and 247-423 □C for 0.01, 0.1 and 5% MBA crosslinker). Again, third and fourth degradation steps are similar for different crosslinker concentarions (about 400-538 and 661-1000 □C).

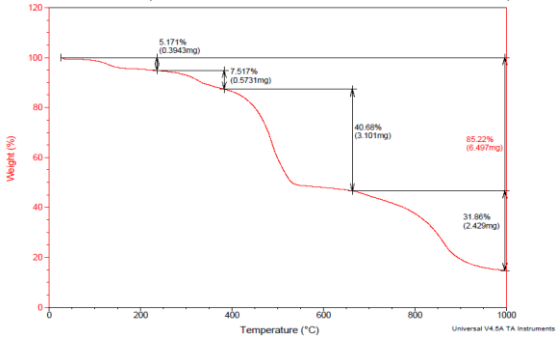

Figure 14: Thermogram for 100/5 weight artion of PNMA/Mag-OA and 0.1% MBA

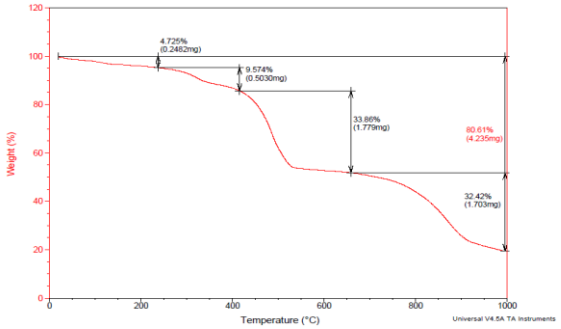

Figure 15: Thermogram for 100/5 weight artion of PNMA/Mag-OA and 5% MBA

For PNMA/G and PNMA/CG NCs, thermograms (not represented here) show advanced thermal stability compared to PNMA/OG NCs. Both first and last step degradation are similar whereas the second and third steps show enhanced stability by a factor of about 50 □C. This enhancement may be attributed to the hydrophilization of the nanoparticles -without modification or with citric acid- enhances their encapsulation by making them compatible with the polymeric matrix.

IV. CONCLUSIONS

Present article presents preparation of non-functionalized and citric acid coated hydrophilic magnetite nanoparticles in addition to hydrophobic oleic acid coated one. Microemulsion polymerization technique was optimized for preparing nanocomposites of poly (sodium methacrylate)/different magnetite types. Such protocol affords nanocomposites with high molecular weight and improved thermal stability that would have promising effect in enhanced oil recovery application.

REFERENCES

[1] K.S. Sorbie, *Polymer-improved oil recovery*, Glasgow, Blackie, Boca Raton, Fla: CRC Press; 1991.

[2] D. Hunkeler, Synthesis and characterization of high molecular weight water-soluble polymers, *Polym. Int*. 1992, *27(1*), 23-33.

[3] C. Ignác, On inverse miniemulsion polymerization of conventional water-soluble monomers, *Adv. Colloid Interface Sci.* 2010, *156(1-2)*, 35–61.

[4] Z.X. Zhang, Z.S. Han, and K.Y. Liu , Study on the synthesis of anionic polyacrylamide under pilot-plant test by inverse suspension copolymerization , *J. Beijing Univ. Chem. Technol.* 2001, *28(1)*, 52-55.

[5] Y.D. Luo, C.A. Dai, and W.Y. Chiu, Polystyrene/Fe3O4 composite latex via miniemulsion polymerization-nucleation

mechanism and morphology, *J. Polym. Sci.*, Part A: Polym. Chem. 2008, *46(3)*, 1014-1024.

[6] J. Zhou, S.W. Zhang, X.G. Qiao, X.Q. Li, and L.M. Wu, Synthesis of SiO2/poly(styrene-*co*-butyl acrylate) nanocomposite microspheres via miniemulsion polymerization, *J. Polym. Sci.*, Part A: Polym. Chem. 2006, *44(10)*, 3202-3209.

[7] G.H. Al-Ghamdi, E.D. Sudol, V.L. Dimonie, and M.S. El-Aasser, Encapsulation of titanium dioxide in styrene/*n*-butyl acrylate copolymer by miniemulsion polymerization, *J. Appl. Polym. Sci.* 2006, *101(5)*, 3479-3486.

[8] S. Sepeur, B. Werner, and H. Schmit, UV curable hard coatings on plastics, *Thin Solid Films* 1999, *351(1-2)*, 216-219.

[9] B. Jiang, and G. Huang, Graft polymerization on magnesium oxide surface, *Radiat. Phys. Chem.* 2004, *69(5)*, 433-438.

[10] R. Zolfaghari, A.A. Katbab, J. Nabavizadeh, R.Y. Tabasi, and M.H. Nejad, Preparation and characterization of nanocomposite hydrogels based on polyacrylamide for enhanced oil recovery applications, *J. Appl. Polym. Sci.* 2006, *100(3)*, 2096–2103.

[11] P. Tongwa, R. Nygaard, and B. Bai, Evaluation of a nanocomposite hydrogel for water shut-off in enhanced oil recovery applications: Design, synthesis, and characterization, *J. Appl. Polym. Sci.* 2013, *128(1)*, 787-794.

[12] S. Si, C. Li, X. Wang, D.Yu, Q. Peng, and Y. Li, Magnetic Monodisperse Fe3O4 Nano particles *Cryst. Growth Des.* 2005, *5(2)*, 391-393.

[13] S.H. Sun, H. Zeng, D.B. Robinson, S. Raoux, P.M. Rice, S.X. Wang, and G.X. Li, Monodisperse MFe2O4 (M = Fe, Co, Mn) Nanoparticles, *J. AM. CHEM. SOC.* 2004, *126(1)*, 273-279.

[14] R.M. Cornell, and U. Schwertmann, , *The Iron Oxides: Structure, Properties, Reactions, Occurences and Uses*, 2nd ed., Wiley-VCH Verlag GmbH & Co. KGaA, Weinheim, 2003.

[15] S. Odenbach, *Ferrofluids: Magnetically Controllable Fluids and Their Applications*, Springer-Verlag, Heidelberg, 2002, pp. 236–242.

[16] A. Wooding, M. Kilner, D.B. Lambrick, Studies of the double surfactant layer stabilization of water-based magnetic fluids, *J. Colloid Interface Sci.* 1991, *144(1)*, 236-242.

[17] M. Ma, Y.Zhang, W.Yu, H. Shen, H. Zhang, and Gu, N., Preparation and characterization of magnetite nanoparticles coated by amino silane, *COLLOIDS SURF.*, A 2003, *212(2-3)*, 219-226.

[18] W. Cai, and J. Wan, Facile synthesis of superparamagnetic magnetite nanoparticles in liquid polyols, *J. Colloid Interface Sci.*, 2007, *305(2)*, 366-370.

[19] L.H. Dubois, B.R. Zegarski, and R.G. Nuzzo, Spontaneous organization of carboxylic acid monolayer films in ultrahigh vacuum. Kinetic constraints to assembly via gas-phase adsorption, *Langmuir* 1986, *2(4)*, 412-417.

[20] I.C. McNeill, M. Zulfiqar, Preparation and degradation of salts of poly(methacrylic acid). I. Lithium, sodium, potassium, and caesium salts, *J. Polym. Sci.*, Part A: Polym. Chem. 1978, *16(12)*, 3201-3212.